

# Extrusion of Alkenes from Rhenium(V) Diolates: The Effect of Substitution and Conformation

Kevin P. Gable,\*<sup>1</sup> and Jerrick J. J. Juliette

Contribution from the Department of Chemistry, Oregon State University, Corvallis, Oregon 97331-4003

Received July 14, 1994<sup>®</sup>

**Abstract:** The kinetics of alkene extrusion from several diolates of the type Cp\*Re(O)(diolate) are measured. The data show that successive methyl substitution increases the activation enthalpy for this process by approximately 1 kcal/mol per methyl group. Reaction rates and  $\Delta G^\ddagger$  also reflect substantial differences in  $\Delta S^\ddagger$ , which are attributed to differences in the average conformation of the diolate ring. Support for this view is seen in conformational analysis of the ring, performed by examining  $^1\text{H}$  NMR coupling constants. The data suggest the extrusion is inhibited if the ring is flat and promoted if it is highly puckered. This agrees with a mechanism involving migration of carbon from oxygen to rhenium, followed by loss of alkene.

Extrusion of alkenes from rhenium(V) diolates is a process that has interested us recently due to the analogy of its microscopic reverse to oxidation of alkenes by metal oxo complexes.<sup>2</sup> The reaction has been observed for a number of different complexes<sup>3</sup> including a system pioneered by Herrmann and co-workers.<sup>4</sup> As part of our effort to understand the mechanism of this process, we undertook a study of the effect of substitution of the diolate ring on the energetics of cycloreversion. We report here the results of this study.

## Results

**Kinetics.** Diolates 1–9 (see Chart 1) were dissolved in  $\text{C}_6\text{D}_6$  and sealed in NMR tubes under vacuum. Upon heating they slowly formed alkene and  $\text{Cp}^*\text{ReO}_3$ . The kinetics of these reactions were followed by  $^1\text{H}$  NMR. Although pure diastereomers (syn and anti) could not be separated for 2, 3, and 8–10, the Cp\* signals were clearly separated in the NMR spectrum and could be followed separately. The Cp\* signals for syn and anti isomers of 7 were not separated, but the syn/anti ratio (as determined by signals from diolate ring protons) was constant throughout the reaction; thus, the rate of reaction of the two isomers was assumed to be identical within experimental uncertainty ( $\pm 3\%$ ). No other byproducts or intermediates were seen; the detection limit was estimated at 1% of the mixture. All compounds showed clean first-order behavior to more than 4 half-lives. Rate constants are listed in Table 1. Data for 1 and 4 and norbornane-2,3-diolate 11 have been reported in ref 2b. Activation parameters calculated from the Eyring equation are listed in Table 2.

**Solution Structure and Conformational Analysis.** Earlier studies by Herrmann<sup>5</sup> clearly showed that the diolate ring of 1 was puckered. Examination of the  $^1\text{H}$  NMR spectrum, particularly of the coupling constants within the diolate ring, reveals

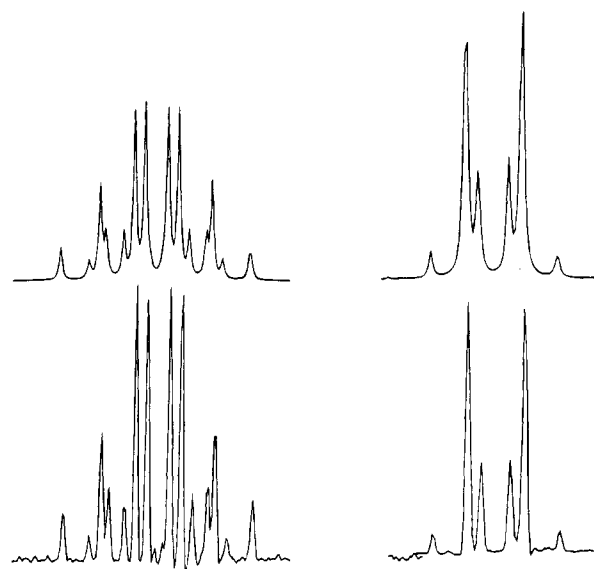


**Figure 1.** Experimental and simulated spectra for 3a. Left: Calculated (top) and experimental (bottom) spectra for the carbinol CH signal (3.74 ppm). Right: Calculated (top) and experimental (bottom) spectra for the methyl signal (1.42 ppm).

this to be the case. The equivalence of the methyl groups and/or of the carbinol CH protons in 1, 3, 5, 8, 9, and 10 shows that two forms are interconverting rapidly at room temperature; cooling a sample of 6 to 204 K showed no decoalescence of either methyl signal. The barrier to ring inversion (assuming a difference in chemical shifts for the low-temperature limit of 0.5 ppm, or 200 Hz) is thus less than 10 kcal/mol. However, cooling cyclohexanediolate 8 to 196 K caused decoalescence of the carbinol CH signal, although the low-temperature limit was not achieved. Again assuming a maximum  $\Delta\delta$  of 200 Hz,  $\Delta G^\ddagger \approx 9.0$  kcal/mol.

Table 3 shows the measured vicinal coupling constants for several of these diolates. For the monosubstituted diolates, identification of this parameter is straightforward; decoupling experiments allowed complete assignment of the spectra. The complexity of the spectrum for 1 and 3a was such that simulation was required to extract the coupling constants; experimental and calculated spectra for 3a are shown in Figure 1. The identity of the virtual coupling between syn protons in 1 was confirmed with a phase-sensitive COSY two-dimensional

<sup>®</sup> Abstract published in *Advance ACS Abstracts*, January 1, 1995.

(1) Internet: gablek@ccmail.orst.edu

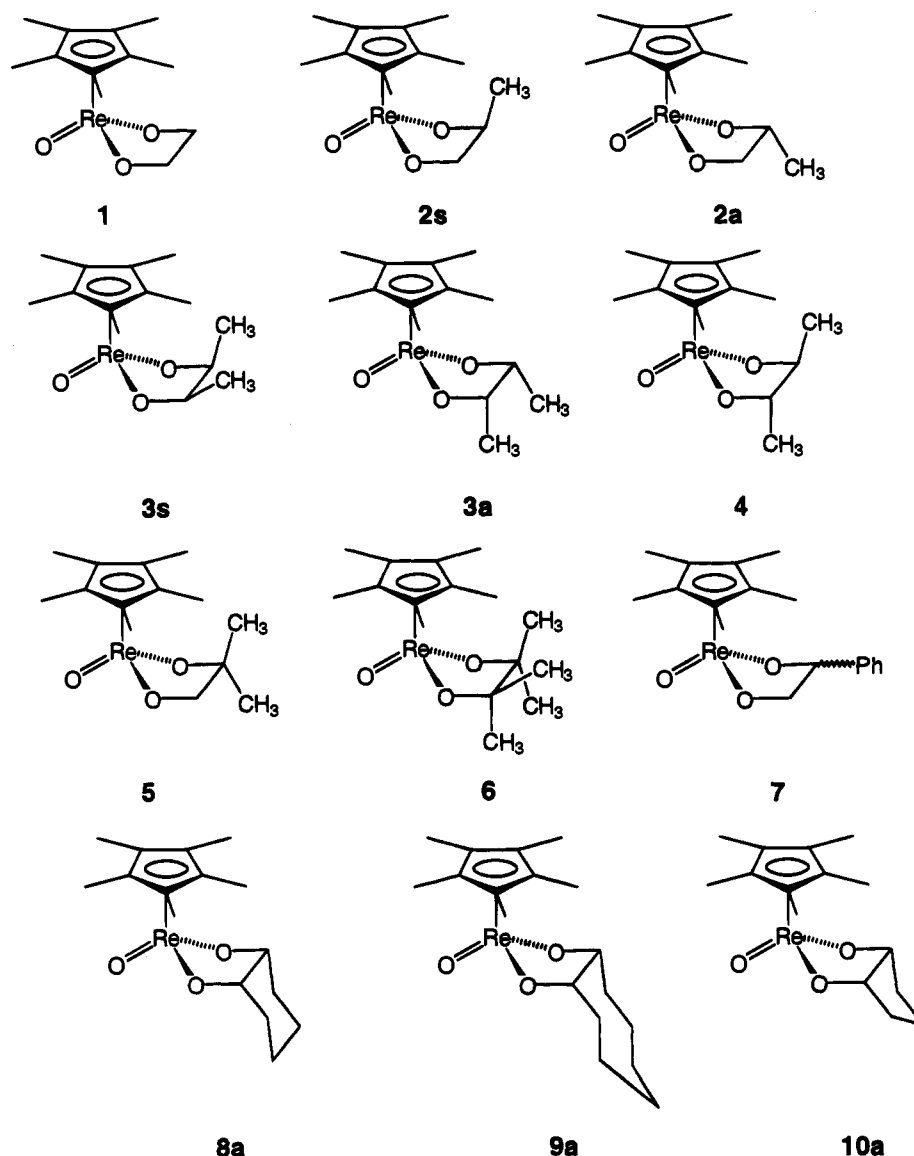
(2) (a) Gable, K. P.; Phan, T. N. *J. Am. Chem. Soc.* **1993**, *115*, 3036–3037. (b) Gable, K. P.; Phan, T. N. *J. Am. Chem. Soc.* **1994**, *116*, 833–839.

(3) (a) Pearlstein, R. M.; Davison, A. *Polyhedron* **1988**, *7*, 1981–1989. (b) Brown, S. N.; Mayer, J. M. *Inorg. Chem.* **1992**, *31*, 4091–4100. (c) Bohm, G.; Weighardt, K.; Nuber, B.; Weiss, J. *Angew. Chem., Int. Ed. Engl.* **1990**, *29*, 787–789.

(4) Herrmann, W. A.; Marz, D.; Herdtweck, E.; Schaefer, A.; Wagner, W.; Kneuper, H.-J. *Angew. Chem.* **1987**, *99*, 462–464.

(5) Herrmann, W. A.; Marz, D. W.; Herdtweck, E. *J. Organomet. Chem.* **1990**, *394*, 285–303.

Chart 1. Diolates Used in This Study



spectrum, showing the (passive) vicinal coupling to be 5.8 Hz. Coupling constants for 8–10 were assigned by selective decoupling of the adjacent methylene protons; assignment was aided by a COSY spectrum.

These parameters were analyzed using a Karplus relationship including treatment of the electronegativity of the oxygen substituents;<sup>6</sup> this allowed an estimation of the time-averaged

(6) Haasnoot, C. A. G.; de Leeuw, F. A. A.; Altona, C. *Tetrahedron* **1980**, *36*, 2783–2792. This paper describes a number of slightly different Karplus curves, but we find only minor disagreement among them; calculated dihedral angles differ by less than 10°, and more importantly, the relationship from one geometry to the next is identical, regardless of the choice of the Karplus model. We used the curve originally calculated by Pachler: Pachler, K. G. R. *J. Chem. Soc. Perkin Trans. II* **1972**, 1936–1940; see Supplementary Material. A referee has objected to this “backwards” treatment of the Karplus relationship, on the basis that without absolute knowledge of the number and geometry of the conformations involved, it is not possible to quantitatively arrive at a true time-averaged structure. However, the diolate rings restrict the O–O dihedral and thus the cis-vicinal H–H dihedral present in all substrates except 4 to less than 60°. Any cis-vicinal H–H coupling constant greater than ca. 3 Hz (the expected coupling for a 60° H–H dihedral) must arise from contribution of a geometry with a dihedral less than 60°, in other words, a more flattened ring. Whether the ground state is slightly flattened to produce the observed NMR behavior or whether there is one or more highly flattened conformers that contributes to the overall structure does not alter our eventual conclusions. These are based on the degree of net deviation from the staggered geometry, and either of the above phenomena will contribute to this.

geometry of the diolate. Where the magnitude of the coupling constant was consistent with two possible dihedral angles, those giving a self-consistent geometric model were chosen (wherein the geminal dihedral angles of the carbinol carbon were assumed to be 120°).

## Discussion

The major contending hypotheses for formation of C–O bonds in reactions of OsO<sub>4</sub> include Criegee’s concerted, [3 + 2] cycloaddition,<sup>7,8</sup> and a stepwise, [2 + 2] mechanism initially put forth by Sharpless.<sup>9</sup> Our interest in cycloreversion of rhenium diolates stems from this controversy, as the reaction we are examining is formally the microscopic reverse of osmylation. Our earlier work<sup>2</sup> indicated the concerted pathway was inconsistent with the energetics of the reaction as a function of alkene strain (Scheme 1, path A). A principal result was that strain in the developing alkene had no apparent effect on

(7) (a) Criegee, R. *Justus Liebigs Ann. Chem.* **1936**, *522*, 75–96. (b) Criegee, R.; Marchand, B.; Wannowius, H. *Justus Liebigs Ann. Chem.* **1942**, *550*, 99–133.

(8) (a) Corey, E. J.; Jardine, P. D.; Virgil, S.; Yuen, P.-W.; Connell, R. D. *J. Am. Chem. Soc.* **1989**, *111*, 9243–9244. (b) Corey, E. J.; Noe, M. C.; Sarshar, S. *J. Am. Chem. Soc.*, **1993**, *115*, 3828–3829. (c) Corey, E. J.; Noe, M. C. *J. Am. Chem. Soc.* **1993**, *115*, 12579–12580. (d) Schröder, M. *Chem. Rev.* **1980**, *80*, 187–213.

Table 1. Kinetics of Alkene Extrusion

compd	alkene	T, K	rate constant, 10 <sup>-5</sup> s <sup>-1</sup>	compd	alkene	T, K	rate constant, 10 <sup>-5</sup> s <sup>-1</sup>
2s	propene	355.0	0.464	8s	cyclohexene	360.4	0.091
		361.8	0.978			369.9	0.297
		367.8	2.00			377.6	0.78
		372.8	3.38			385.0	1.80
		378.0	6.27			388.6	2.52
2a	propene	385.1	12.4	8a	cyclohexene	360.4	0.095
		355.0	0.454			369.9	0.324
		361.8	1.06			377.6	0.73
		367.8	2.00			385.0	1.88
		372.8	3.39			388.6	2.87
3s	(Z)-2-butene	378.0	6.22	9s	cis-cyclooctene	322.9	0.213
		385.1	12.9			330.6	0.57
		355.0	0.226			338.0	1.69
		361.8	0.525			339.9	1.62
		367.8	0.919			343.6	2.84
3a	(Z)-2-butene	377.8	3.19	9a	cis-cyclooctene	353.7	8.36
		385.1	6.93			360.4	17.8
		355.0	0.221			322.9	0.220
		361.8	0.527			330.6	0.62
		367.8	1.10			338.0	1.87
5	2-methylpropene	377.8	3.24	10s	cyclopentene	339.9	1.85
		385.1	7.94			343.6	3.13
		359.2	0.386			353.7	9.52
		364.6	0.728			360.4	20.5
		367.8	1.06			347.7	0.32
6	2,3-dimethyl-2-butene	377.6	3.35	10a	cyclopentene	358.1	1.03
		385.2	7.85			368.1	3.30
		390.0	12.2			372.7	4.65
		398.8	29.8			378.9	7.90
		358.0	0.289			347.7	0.37
7	styrene	364.6	0.637			358.1	1.21
		371.6	1.52			368.1	3.60
		378.0	3.50			372.7	6.22
		385.2	7.45			378.9	11.0
		390.0	12.5				

Table 2. Activation Parameters for Alkene Extrusion

compd	alkene	$\Delta H^\ddagger$ <sup>a</sup>	$\Delta S^\ddagger$ <sup>a</sup>
2s	propene	29.2 ± 0.4	-1.0 ± 1.0
2a	propene	29.3 ± 0.3	-0.7 ± 0.9
3s	(Z)-2-butene	30.2 ± 1.0	0.3 ± 2.8
3a	(Z)-2-butene	31.2 ± 0.6	3.3 ± 1.7
5	2-methylpropene	30.7 ± 0.3	1.7 ± 0.7
6	2,3-dimethyl-2-butene	32.3 ± 0.4	6.0 ± 1.1
7	styrene	26.1 ± 0.1	0.6 ± 0.1
8s	cyclohexene	32.6 ± 1.0	3.9 ± 2.8
8a	cyclohexene	32.7 ± 0.9	4.3 ± 2.4
9s	cis-cyclooctene	26.4 ± 0.6	-2.8 ± 1.7
9a	cis-cyclooctene	27.0 ± 0.6	-0.9 ± 1.8
10a	cyclopentene	28.8 ± 0.7	-1.2 ± 1.5
10s	cyclopentene	26.7 ± 0.9	-7.4 ± 2.0
4 <sup>b</sup>	(E)-2-butene	30.5 ± 0.5	-0.8 ± 1.1
1 <sup>b</sup>	ethylene	28.0 ± 0.4	-2.1 ± 1.2
11 <sup>b</sup>	norbornene	29.1 ± 0.5	-7.2 ± 1.8

<sup>a</sup> Units for  $\Delta H^\ddagger$  are kcal/mol; those for  $\Delta S^\ddagger$  are cal/(mol·K). Uncertainties are expressed as 95% confidence limits. <sup>b</sup> From ref 2b.

activation enthalpy, excluding a mechanism where sp<sup>2</sup> character was developing at the reacting carbon. The observation of a

(9) (a) Sharpless, K. B.; Teranishi, A. Y.; Bäckvall, J.-E. *J. Am. Chem. Soc.* **1977**, *99*, 3120–3128. (b) Hentges, S. G.; Sharpless, K. B. *J. Am. Chem. Soc.* **1980**, *102*, 4263–4265. (c) Gobel, T.; Sharpless, K. B. *Angew. Chem., Int. Ed. Engl.* **1993**, *32*, 1329–1331. (d) Kolb, H. C.; Andersson, P. G.; Bennani, Y. L.; Crispino, G. A.; Jeong, K.-S.; Kwong, H.-L.; Sharpless, K. B. *J. Am. Chem. Soc.* **1993**, *115*, 12226–12227. (e) Kolb, H. C.; Andersson, P. G.; Sharpless, K. B. *J. Am. Chem. Soc.* **1994**, *115*, 1278–1291.

Table 3. Diolate Ring Vicinal Coupling Constants and Calculated Dihedral Angles

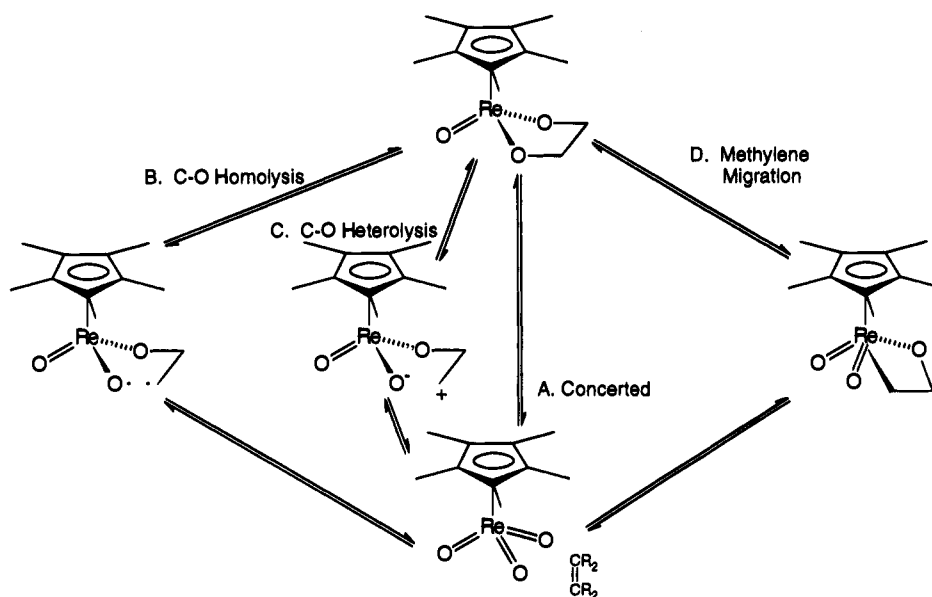
compd	coupling constant	calcd HCCH angle <sup>6</sup>	compd	coupling constant	calcd HCCH angle <sup>6</sup>
7s	10.1	159	3s	5.3	38
	5.7	35		1	5.8
7a	8.8	148	8a	3.6	50
	6.6	26		9a	5.1
2s	9.9	157	9s	3.9	50
	5.5	36		10a	5.0
4	8.9	149	10s	7.9	3
3a	5.3	38			

significant secondary deuterium isotope effect also implied substantial reorganization of the bonding to this carbon during the rate-determining step. The electronic effect of alkyl substitution also argued against formation of an electron deficient carbon in the initially-formed intermediate (paths B and C).<sup>10</sup> Our results were consistent with rate-determining formation of a metallaoxetane (path D) in that there is a change in bonding to carbon without rehybridization to sp<sup>2</sup>. However, the work gave no positive evidence for the structure of this intermediate. Consequently, we undertook a systematic study of substituent effects to more fully characterize the rate-determining step in the diolate cycloreversions.

The comparison of rate constants at 104–105 °C shows several notable features. First, there is no difference, within

(10) (a) Wallis, J. M.; Kochi, J. K. *J. Am. Chem. Soc.* **1988**, *110*, 8207–8223. (b) Wallis, J. M.; Kochi, J. K. *J. Org. Chem.* **1988**, *53*, 1679–1686.

Scheme 1



experimental error, in the rates of cycloreversion of **3s** and **3a** or between **2s** and **2a**. The activation parameters for these pairs of reactions also show no significant differences. One possible explanation is that the two isomers interconvert rapidly under the reaction conditions, and that one reacts preferentially. We have not been successful either in isolating pure isomers or in generating significantly different mixtures of isomers of **3** (chromatography, fractional crystallization, equilibration with excess diols at elevated temperatures),<sup>11</sup> so we must conclude that rapid equilibration of stereoisomers might occur. Surprisingly, though, there is no systematic variation of isomeric composition with temperature for any of the compounds studied here; see Table 4. Therefore, if interconversion is rapid under cycloreversion conditions, then each compound *fortuitously* exhibits an equilibrium between isomers that is both unique to each compound and invariant with temperature.<sup>12</sup> Alternatively, if the composition is set during preparation, and interconversion does not occur rapidly under cycloreversion conditions, then the Curtin-Hammett principle does not apply in this instance. We find the latter conclusion more plausible.

This similarity of reaction rates for **3**, **5**, and **6** is quite surprising. At 104–105 °C, each is in the range  $3.2\text{--}3.5 \times 10^{-5} \text{ s}^{-1}$ . Our earlier comparison of ethylene extrusion with that of *trans*-2-butene ( $1.76 \times 10^{-4}$  and  $1.24 \times 10^{-5} \text{ s}^{-1}$ , respectively) demonstrated an apparent deceleration due to the presence of the inductively electron donating methyl groups. One would predict that according to any mechanism, compound **6** should be significantly slower than **3**, **4**, or **5**, assuming that the rate differences are determined primarily by differences in activation enthalpy.

Examination of activation parameters (as opposed to just rate constants) reveals that activation enthalpies for cycloreversion

(11) We have shown that exchange with external diol can occur: ref 26. In the absence of external diol, though, the mechanism for *syn/anti* equilibration remains quite speculative. Cleavage of a C–O bond (e.g., to a carbocation) can be ruled out based on the absence of <sup>18</sup>O scrambling during extrusion of ethylene from labeled **1** (Phan, T. N. M.S. Thesis, Oregon State University, 1993). Cleavage of a Re–O bond is also possible, but given the nonpolar nature of the solvent used (C<sub>6</sub>D<sub>6</sub>) it is also unlikely. A final possibility that would be consistent with rapid interconversion in a nonpolar medium is a Berry-type pseudorotation by which one of the diolate oxygens would rotate through the position trans to the Cp\* ring. Such a process must still be slow on the NMR time scale (we have not observed coalescence of the NMR peaks for the two stereoisomers at temperatures up to 50 °C).

(12) We have examined butanediolate **3** by NMR at 25 and 50 °C and find no significant shift in isomeric composition.

Table 4. Isomeric Composition before and during Cycloreversion

compd	temp, K	anti/syn ratio <sup>a</sup>	
		initially	during reaction (80% conversion)
<b>2</b>	355.0	1.08	1.15
	361.8		1.08
	367.8		1.04
	372.8		1.15
	378.0		1.14
	385.1		1.03
<b>3</b>	355.0	4.20	4.44
	361.8		4.28
	367.8		4.52
	377.8		3.96
	385.1		3.98
<b>8</b>	360.4	5.96	5.85
	369.9		5.68
	377.6		5.47
	385.0		5.55
	388.6		5.52
<b>9</b>	322.9	3.12	3.26
	330.6		3.17
	338.0		3.01
	339.9		3.62
	343.6		2.72
	353.7		3.04
	360.4		2.70

<sup>a</sup> Uncertainties  $\pm 5\text{--}10\%$ .

of methyl-substituted diolates do indeed show a systematic behavior. Each methyl group raises the activation enthalpy by about 1.0 kcal/mol. Other structures showed different trends; the phenyl group lowered  $\Delta H^\ddagger$ , consistent with this group being slightly more electronegative than H.<sup>13</sup> Diolates that extrude cyclic alkenes show a range of activation enthalpies which likely reflect increases or decreases in torsional strain (*vide infra*). The observed rates for each are determined by the interplay of enthalpy and entropy, and for the latter we see variations that require a more detailed consideration of molecular structure.

Herrmann has observed that the crystal structure of the ethanediolate **1** contains a puckered ring.<sup>5</sup> This is consistent with the structure expected for a five-membered metallacycle.

(13) The Hammett constants for a phenyl group are  $\sigma_{\text{para}} = -0.01$ ;  $\sigma_{\text{meta}} = +0.06$ . Ritchie, C. D.; Sager, W. F. *Prog. Phys. Org. Chem.* **1964**, *2*, 323. Recall also that  $sp^2$ -hybridized carbon is more electronegative than  $sp^3$ : Wiberg, K. B.; Bader, R. F. W.; Lau, C. D. H. *J. Am. Chem. Soc.* **1987**, *109*, 1001–1012. Coulson, C. A. *Valence*, 2nd ed.; Oxford University: Oxford, 1961; p 218.

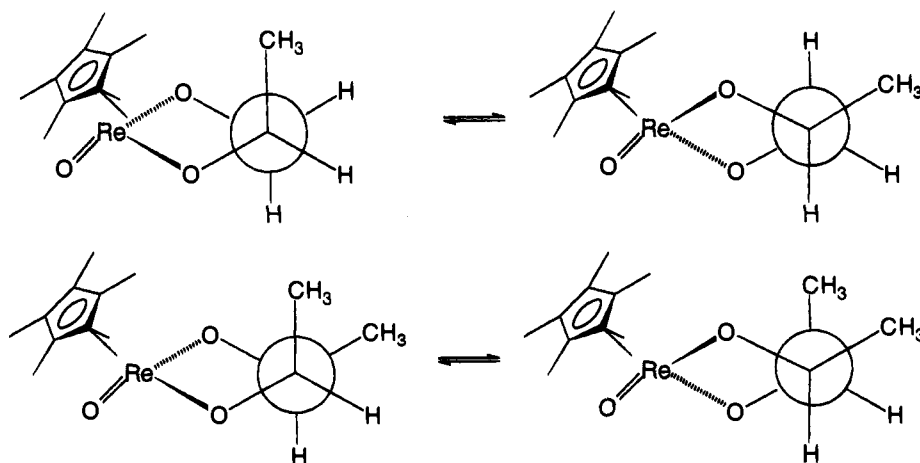


Figure 2. Newman projection of the diolate ring for **2s** and **3s**.

The NMR behavior of the compounds we have examined does not immediately reflect such a structure; **1** shows an AA'BB' pattern, rather than the ABCD pattern predicted from the static structure. However, flipping of the ring interchanges two sets of proton sites, as is seen for **3s** in Figure 2.

Such structures suggest why syn and anti isomers might not show radical differences in reaction rates. In each case, the ring can avoid interaction with the relatively bulky Cp\* ligand by orienting the substituents away from the Cp\* methyl groups. Furthermore, they help rationalize the otherwise puzzling observation that *trans*-2-butene is extruded from **4** at a rate one-third that of *cis*-2-butene extrusion from either isomer of **3**: the disposition of methyl groups of **3** in pseudo-equatorial or pseudo-axial positions is identical, regardless of stereochemistry at rhenium, while that for **4** requires either both methyls be pseudo-axial or both be pseudo-equatorial.

Some of these diolates are readily subject to conformational analysis, since proton-proton coupling constants may be measured in the  $^1\text{H}$  NMR spectrum. This is most easily seen in the phenyl-substituted **7s**, although the behavior in methyl-substituted **2** is qualitatively the same. The syn isomer has the three protons well spread out, and typically shows a large (10.1 Hz) and a small (5.7 Hz) vicinal coupling, in addition to the expected large geminal coupling of  $(-10.8)$  Hz.<sup>14</sup> Analysis of this information according to an appropriate Karplus relationship<sup>6</sup> suggests the two vicinal dihedral angles here are  $35^\circ$  and  $159^\circ$ . An average structure thus places the carbons in the ring such that they are twisted by  $25^\circ$  ( $60^\circ - 35^\circ$ ) from the staggered geometry, as shown in Figure 3. This places the substituent in a pseudo-equatorial position.

The anti isomer displays similar behavior. In the case of propanediolate **2**, all three protons show accidental chemical shift equivalence, and the coupling information cannot be extracted from the high-order spectrum. However, in the phenylethanediate **7a**, the proton at C-1 is well separated, and shows couplings of 8.8 and 6.6 Hz. These best fit a situation where the C-1 proton has dihedral angles of  $26^\circ$  and  $148^\circ$  with the two protons in the methylene group. This picture suggests a twist from the ideal staggered conformation of  $32$ – $34^\circ$  (Figure 3), similar to that for the syn isomer.

A similar analysis can be done for the vicinally disubstituted diolates. The vicinal coupling in the ring of threeo compound **4** is 8.9 Hz, corresponding to a dihedral angle of  $149^\circ$ , or a twist from the ideal staggered geometry of  $31^\circ$  (Figure 3). This supports the assertion made above that this compound prefers

to place both methyl groups in pseudo-equatorial positions. For the erythro isomer **3a**, finding this coupling constant required computer simulation. A good fit was observed when  $J_{23}$  was set to 5.3 Hz, indicating a dihedral angle of  $38^\circ$ , or a twist of  $22^\circ$  from the staggered conformation. Comparison of **3** and **4** shows that *the compound which reacts more slowly has a higher twist away from the staggered geometry, or a more flattened diolate ring.*

It is important to emphasize that the NMR data reveal the average solution structure. For all of these compounds, it is expected that the minimum energy conformation will be staggered; this is supported by molecular mechanics calculations<sup>15</sup> and is also strongly suggested by Herrmann's solid state structures.<sup>5</sup> However, the symmetry seen in the NMR spectra shows these structures are in the process of flipping back and forth, for example, interconverting the two forms of **3s**, similar to what is shown in Figure 2. The "twist" away from staggered geometry suggested by the vicinal coupling constants actually reflects the amount of time the molecule spends in other conformations, rather than a single static structure.

The conclusion that arises from this conformational analysis is that the closer a ring's average conformation to an idealized staggered geometry is (alternatively, the more of the ensemble occupy the staggered conformation), the more positive  $\Delta S^\ddagger$  will be. After examining the range of structures used in this study, we see that, in general, this is the case; a graphical presentation is presented in Figure 4. For compound **11**, extrusion of norbornene from the quite rigid diolate (in which the eclipsed conformation should be seen)<sup>16</sup> shows a very negative activation entropy of  $-7.2$  cal/(mol·K). For pinacolate **6**, where gauche interactions between methyl groups should more rigorously enforce the staggered geometry, we see a distinctly positive value of  $+6.0$  cal/(mol·K). Most of our observations fall between this, but there is a rough correlation between average geometry and activation entropy.

To test this hypothesis, we measured activation parameters for **8**, **9**, and **10**. *cis*-Cyclohexanediate **8** is expected to have the more staggered geometry due to the preference of the cyclohexane ring for a chair geometry. This is, in fact, seen from the vicinal coupling constant of 3.6 Hz for **8a**, corresponding to a dihedral angle of  $50^\circ$ , or a twist from a perfect staggered geometry of  $10^\circ$ .

We observe that extrusion of cyclohexene from **8** is slower than expected. This is due primarily to the high  $\Delta H^\ddagger = 32$ – $33$  kcal/mol, higher than other disubstituted diolates. This

(14) Silverstein, R. M.; Bassler, G. C.; Morrill, T. C. *Spectrometric Identification of Organic Compounds*, 4th ed.; John Wiley & Sons: New York, 1981; p 209.

(15) Hyperchem MM+, Version 3.0. Gable, K. P., unpublished results.  
(16) (a) Angyal, S. J.; Craig, D. C.; Trung, Q. T. *Aust. J. Chem.*, **1984**, *37*, 661–666. (b) Anet, F. A. L. *Can. J. Chem.* **1961**, *39*, 789–794.

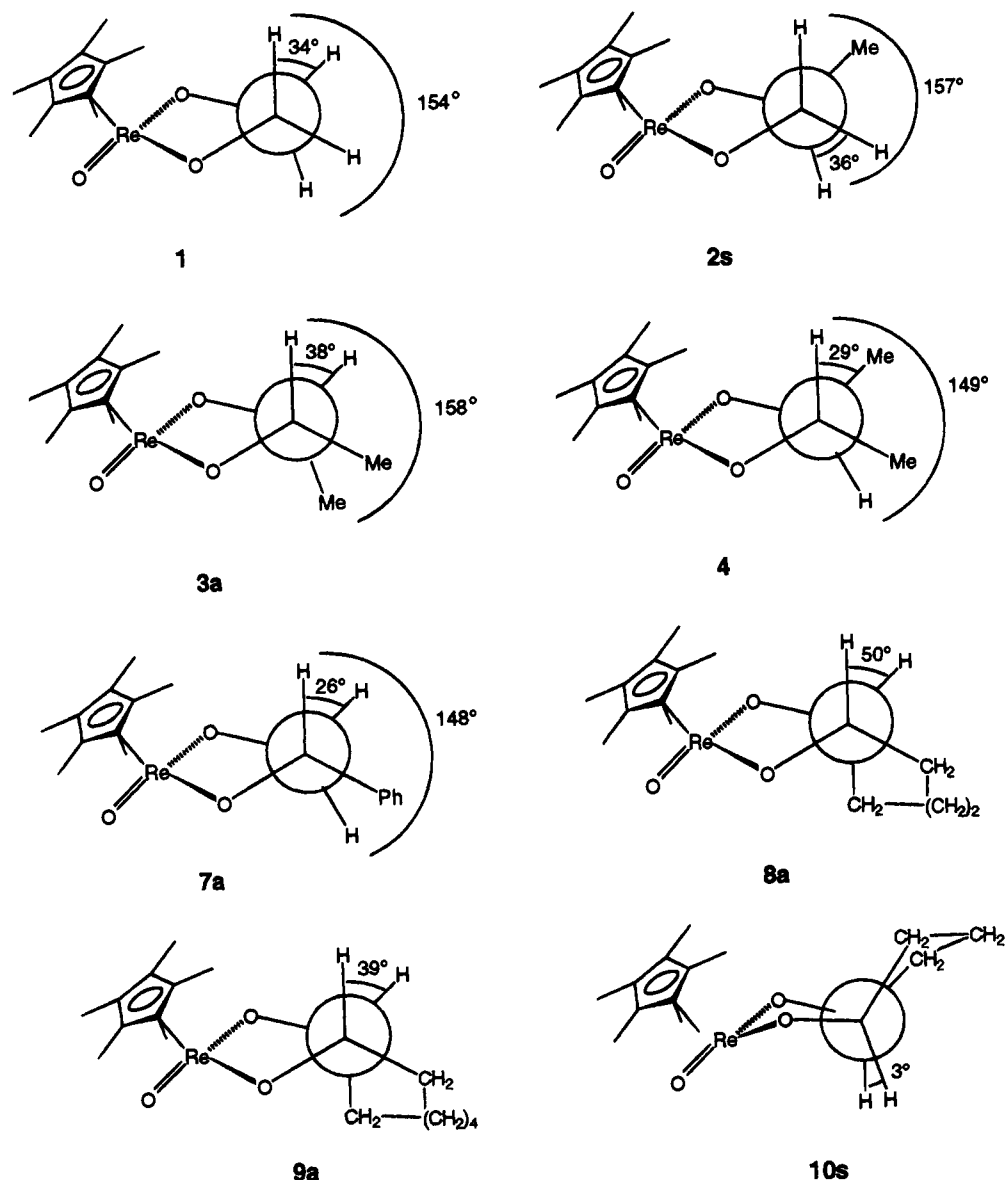


Figure 3. Average solution structures of several diolate rings, based on vicinal coupling constants.

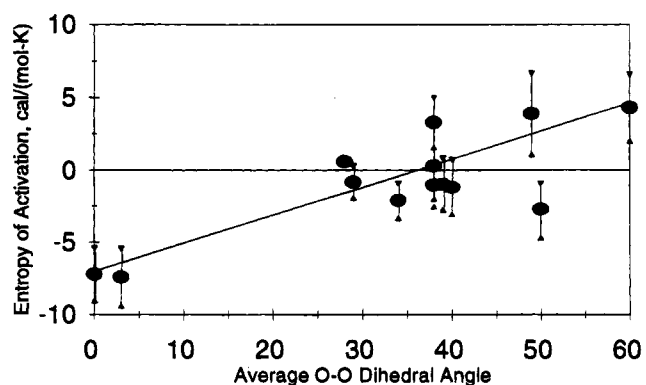


Figure 4. Entropy of activation (including experimental uncertainty) vs. average solution geometry in the diolate ring.

probably reflects torsional strain that develops on distortion of the six-membered ring away from the preferred chair form. However,  $\Delta S^\ddagger = +4.3$  cal/(mol·K), consistent with the expectation based on the low vicinal coupling constant.

In *cis*-cyclooctanediolate **9a**, the coupling constant at room temperature reveals an average twist of  $20^\circ$ , and because of the increased flexibility of the ring in fact  $\Delta S^\ddagger = -0.9$  cal/(mol·K). For extrusion of *cis*-cyclooctene from **9**,  $\Delta H^\ddagger = 26$ – $27$  kcal/

mol, much lower than that for any other vicinally disubstituted olefin. This probably reflects the torsional strain energy present in the saturated 8-membered ring<sup>17</sup> being relieved somewhat in the transition state.

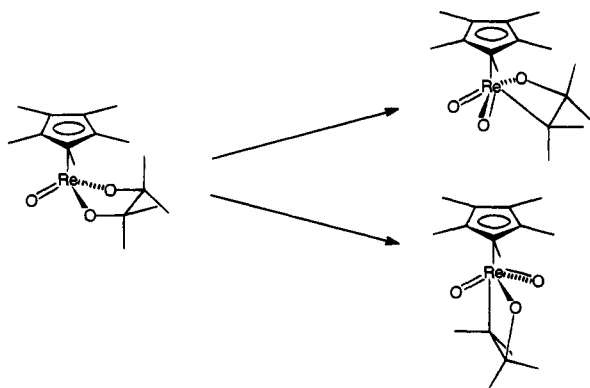
Cyclopentanediolate **10** was selected because molecular mechanics calculations suggested a preference for a small O–O dihedral angle. This is the one example that exhibits dramatic differences in both activation entropies and average conformation for syn and anti isomers. The coupling constant extracted for **10a** (5.0 Hz) corresponded to an average dihedral of  $40^\circ$ , while that for the syn isomer (7.9 Hz) corresponded to a very eclipsed dihedral of  $3^\circ$ . After measuring rate constants for extrusion of cyclopentene, we found low  $\Delta H^\ddagger$  values of 28.8 and 26.7 kcal/mol; presumably these smaller values are due to a release of eclipsing interactions which destabilize the ground state (similar to **9**). The activation entropies, as predicted above from the O–O dihedral angle, were both negative, but the more eclipsed syn isomer was significantly more negative ( $-7.9$  cal/(mol·K)).

Two mechanistic inferences may be drawn from conformational analysis of the diolates. First, it is inconsistent with the hypothesis that these cycloreversions are concerted processes.

(17) Engler, E. M.; Andose, J. D.; Schleyer, P. v. R. *J. Am. Chem. Soc.* **1973**, *95*, 8005–8025.

If these were concerted fragmentations, one would expect that alignment of the C—O bonds would be critical to the development of the incipient C=C  $\pi$  bond. Thus, a flat ring (eclipsing geometry) should promote cycloreversion. That this is not the case is supported by Herrmann's solid state characterization of aza and thia analogs;<sup>5</sup> these rings with better  $\pi$ -donor heteroatoms are flat, yet they cyclorevert very slowly, if at all.<sup>18</sup> In fact, this earlier work specifically posits that the ring conformation controls reactivity; our results support such a view.

A second inference is that alignment of a C—O bond relative to an orbital on rhenium is important for the productive reaction.<sup>19</sup> This suggests a mechanism involving rate-limiting migration of carbon from oxygen to rhenium. One significant question is whether one should expect this to show up as it does in the entropy of activation. An enthalpic component due to steric compression of groups on the migrating carbon may indeed be operating; while we have assigned the increase in  $\Delta H^\ddagger$  with increasing substitution to an electronic effect arising from destabilization of the developing Re—C bond,<sup>2b</sup> there may be a steric component to this effect. It is apparently small, but two factors come into play. The long Re—C bond in the proposed metallaoxetane intermediate minimizes the steric interactions between groups on carbon and other ligands of rhenium. It is also difficult to predict the geometry of this intermediate. Although a four-legged piano stool would be consistent with other Re(V) structures, the metallaoxetane would be formally Re (VII). Structurally related RReO<sub>3</sub> compounds are known to add Lewis bases trans to the aryl R ligand,<sup>20</sup> and such a geometry in the metallaoxetane would also place the substituents at carbon out of the way of any other group except the (sterically undemanding) oxo ligands:



Such a geometry should also be favored in the oxidation of strained alkenes by Cp\*ReO<sub>3</sub><sup>2b</sup> since the approach to rhenium trans to the Cp\* ligand is sterically favorable.

The entropy effect is reasonable if one considers  $\Delta S^\ddagger$  to be due in large part to statistical factors. One can view activation entropy as reflecting the probability that a particular molecule is correctly oriented along the reaction coordinate when it receives collisional activation.<sup>21</sup> The more usual description of entropy effects centers on gain or loss of translational, rotational and vibrational degrees of freedom.<sup>22</sup> The two

(18) The interruption of the  $\pi$  donation needed to achieve proper reaction geometry is also expected to add a significant enthalpic barrier in this process.

(19) Preliminary extended Hückel calculations indicate that the LUMO is a  $d_{z^2}$  type orbital lying along the Re—Cp\* axis; a large lobe of this empty orbital is pointed to the center of the ReO<sub>3</sub> group: Gable, K. P., unpublished results.

(20) De Meric de Bellefon, C.; Herrmann, W. A.; Kiprof, P.; Whitaker, C. R. *Organometallics* **1992**, *11*, 1072–1081.

(21) Moore, J. W.; Pearson, R. G. *Kinetics and Mechanism*, 3rd ed.; John Wiley & Sons: New York, 1981; p 181.

(22) Carey, D. A.; Sundberg, R. J. *Advanced Organic Chemistry*, Part A, 3rd ed.; Plenum: New York, 1990; p 195.

descriptions are easily related, though; if a molecule has a large number of degrees of freedom in the ground state (e.g., sigmatropic rearrangements in medium to large rings), then a collection of such molecules will occupy a large number of conformations. The probability of a particular member of this collection reacting after collisional activation is low, and  $\Delta S^\ddagger$  will be quite negative. Conversely, if a molecule gains degrees of freedom as it reacts (e.g., in fragmentations of cyclic azo compounds), then by definition there is a high probability that a conformationally constrained compound will react when collisionally activated, and thus it will show a positive  $\Delta S^\ddagger$ . Structural changes to the molecule resulting in modification in the degrees of freedom in the ground state will also cause changes in activation entropy for any particular reaction.

A more formal description is to recall the Boltzmann equation for entropy,<sup>23</sup>

$$S = \kappa \ln \Omega \quad (1)$$

where  $\Omega$  is the number of available microstates. Activation entropy is thus expressed as

$$\Delta S^\ddagger = \kappa \ln(\Omega^\ddagger/\Omega^\circ)$$

where  $\Omega^\ddagger$  is the number of microstates available to the activated complex, and  $\Omega^\circ$  is the number available to the ground state. In our case, the necessary alignment of the migrating C—O bond limits  $\Omega^\ddagger$ . Variations in ground state geometry reflected in the average solution structure imply differences in  $\Omega^\circ$  for different molecules, and thus variation of  $\Delta S^\ddagger$  with structure.

It is difficult to find a direct literature analogy to this entropy effect. However, it is well documented that where orientation is important to a reaction, significant conformational effects on rate are seen. A good example is the E2 elimination of trialkylcycloalkylammonium chlorides.<sup>24</sup> Here, the rate of elimination in medium membered rings shows a 10-fold decrease in rate as the ring size is increased from 7 to 12 carbons. This occurs for formation of both cis alkene (thought to occur via anti elimination) and trans alkene (thought to occur via syn elimination). Although activation parameters have not been determined for these processes, it is tempting to rationalize the result on the basis of increased conformational flexibility in the larger rings, decreasing the proportion of molecules in the correct conformation. However, it is not possible to rule out enthalpic effects in this example, and solvation effects will certainly make a large contribution which may vary as a function of ring size.

There are some important limitations to this argument. First, one must be cautious about interpreting activation entropies due to the inherent experimental uncertainty in this measurement and in the assumptions of transition-state theory.<sup>25</sup> Were this entropy effect the only data available, it would be imprudent to claim it definitively distinguished among the mechanistic

(23) McQuarrie, D. A. *Statistical Thermodynamics*; Harper & Row: New York, 1973; pp 55–57.

(24) (a) Saunders, W. H., Jr.; Cockerill, A. F. *Mechanisms of Elimination Reactions*; Wiley-Interscience: New York, 1973. (b) Sicher, J.; Závada, J.; Krupička, J. *Tetrahedron Lett.* **1966**, 1619–1625. (c) Sicher, J.; Závada, J. *Collect. Czech. Chem. Commun.* **1968**, *33*, 1278–1293.

(25) An appropriate caution about assigning structural significance to the measured entropy of activation may be found in: Benson, S. W. *The Foundations of Chemical Kinetics*; McGraw-Hill: New York, 1960; pp 251–252. However, we note that many of the factors which make structural interpretation of a single activation entropy imprudent tend to cancel out during a comparison of a group of related examples. The weakness of the non-quantum mechanical model for reactivity, identity of the frequency factor with a specific normal mode, or the magnitude of the actual frequency factor compared to  $\kappa T/h$  will affect the quantitative validity of the transition state theory expression for the rate constant, but the degree to which they do so should be about the same for any series of structurally similar substrates.

alternatives. However, in light of earlier results for this system, it does reinforce and support the concept of a metallaoxetane intermediate. In addition, we have attempted to use as wide a temperature range as practical for each compound used in our investigation and have examined a reasonably large number of examples.

The rate constant for each substrate is determined by an interplay of enthalpy and entropy terms, as one should expect. While the enthalpies of activation can be interpreted in a straightforward manner, several contributors other than average conformation may also contribute to the activation entropies. One is the effect of solvation; although variation in this should be minor (given the nonpolar nature of the benzene solvent), there will still be some solvent reorganization on going to the transition state that may vary with structure. One estimate of how significant this variation may be is the difference in  $\Delta S^\ddagger$  for **1**, **2s**, and **3a**, which have very similar average diolate geometries, but span a range of 5 cal/(mol·K) in activation entropy. However, this is smaller than the total range we see (13 cal/(mol·K)), and does not detract from the overall trend seen in Figure 4.

The validity of our structural evaluation is limited by the quality of the NMR data. The likely uncertainty in measured coupling constants is  $\pm 0.5$  Hz, taking into account the line widths and digital resolution of our spectra. However, it is pleasing to note that changing the *cis*-vicinal coupling constant (from which we draw our conformational data) by this much leads to a significant degradation of the fit from simulation of the peak pattern. Consequently, we conclude that while the absolute values for the calculated dihedral angle may be in error, the *relative* values (on which the above arguments are based) are much more reliable than the  $\pm 20$ – $30^\circ$  associated with a 1-Hz uncertainty in coupling constant. As a predictive tool, Figure 4 suggests that most diolates will have average geometries that result in near-zero activation entropies. Only when a system becomes "locked" into a staggered or eclipsed conformation will it show a dramatically positive or negative  $\Delta S^\ddagger$ .

Finally, we must consider the impact of the Curtin–Hammett principle on our conclusions. If indeed the *syn* and *anti* isomers are in rapid equilibrium (despite arguments to the contrary), then it is possible that a single transition state for both isomers may not reflect the structural information gleaned from the diolate. Two pieces of evidence mitigate this argument. First, for every set of isomeric diolates except **10s** and **10a**, the vicinal coupling constants are almost identical, suggesting very similar diolate ring conformations. Given the close energetic similarity of isomeric diolates ( $\Delta G^\circ < 1$  kcal/mol), it is reasonable to expect that transition states arising from each will also be close in energy. Thus reaction energetics will be controlled by ground state phenomena. Second, the only set to exhibit different average conformations (**10**) is also the one set to exhibit reactivity differences, and these relative reactivities fit the overall trend for all other compounds. Our interpretation of the reaction energetics suggests that ground state behavior controls reactivity, and reversible interconversion of isomeric reactants does not modify this conclusion.

Faced with the various mechanistic alternatives in Scheme 1, we arrive at the choice between a concerted retro-[3 + 2] process and formation of a metallaoxetane due both to the stereospecificity of the process and to the substituent effect of alkyl substitution. The concerted hypothesis continually generates expectations at odds with observed behavior. On the other hand,

the proposed intermediacy of a metallaoxetane produces a consistent picture. Consequently, our current results add to the weight of evidence supporting this intermediate in cycloreversion of these rhenium diolates, and further restrict the topology of any other potential structure which has yet to be suggested.

## Conclusion

Conformational analysis of rhenium(V) diolates of the type Cp\*Re(O)(diolate) confirms that these adopt a staggered geometry, and that different conformational forms are in rapid equilibrium. The average solution structure varies as a function of substituent(s), and this has a significant effect on the reactivity of the diolate toward cycloreversion. As the ring flattens in the *average* structure, the molecule becomes less likely to adopt the necessary conformation to react, and the entropy of activation for the cycloreversion becomes more negative and the fragmentation becomes slower. Conversely, substituents which promote staggered geometry cause the entropy of activation to become more positive, and increase the rate of reaction. These rate changes are independent of electronic and steric substituent effects, which are reflected in the enthalpy of activation. These results are inconsistent with a concerted mechanism for cycloreversion, but consistent with rate-determining formation of a metallaoxetane by migration of carbon from oxygen to rhenium.

## Experimental Section

All manipulations were performed using standard inert-atmosphere techniques in a nitrogen-filled glovebox (Vacuum Atmospheres Co. HE 493) or on a double-manifold Schlenk line. Benzene-*d*<sub>6</sub> was distilled from sodium benzophenone ketyl. NMR spectra were obtained on either a Bruker AC300 (operating at 300.133 MHz for proton, or 75.469 MHz for <sup>13</sup>C) or a Bruker AM400 (operating at 400.134 MHz for proton, or 100.614 MHz for <sup>13</sup>C) spectrometer. A 30 s relaxation delay was used in collecting NMR data to ensure accurate integration.

Preparation of compounds **1**–**7** is described in an earlier report;<sup>26</sup> compounds **8**–**10** were prepared using this same methodology. These new compounds showed the expected spectra and gave satisfactory elemental analyses.<sup>27</sup> Samples for kinetic analysis were prepared by dissolving the diolate in C<sub>6</sub>D<sub>6</sub>, transferring the solution to an NMR tube, and sealing the tube under vacuum. Kinetics were performed as described earlier,<sup>2b</sup> and each run was followed to at least 3, and normally more than 4 half-lives. All reactions showed clean first-order behavior.

Simulation of NMR spectra was performed using the PANIC program from Bruker Instruments. Initial estimates were made for each coupling, and the program was allowed to optimize each for a best fit to the observed spectrum. Root-mean-square error was less than 0.5%.

**Acknowledgment.** Support from the National Science Foundation (Grant No. CHE-931650) is gratefully acknowledged.

**Supplementary Material Available:** Synthetic procedures and characterization of new compounds **8**, **9**, and **10**, graphical representation and statistical analysis of Eyring plots for diolate cycloreversions, and description of the Karplus functions used to interpret vicinal coupling constants (5 pages). This material is available in many libraries on microfiche, immediately follows this article in the microfilm version of the journal, and can be ordered from the ACS; see any current masthead page for ordering information.

JA942289O

(26) Gable, K. P. *Organometallics* **1994**, *13*, 2486–2488.

(27) See Supplemental Material for details of preparation and characterization.